

1 **(1) comments from referees/public is written in bold type.**

2 (2) author's response is written in normal type.

3 *(3) author's changes in the manuscript is written in italic red type.*

4

5 Reply to Referee Comment #1 (RC1)

6 Thank you for your feedback and suggested revisions. We would also like to
7 thank you for the many useful references you provided us with. We appreciate
8 your time and effort in reviewing our preprint.

9 We have considered the comments and taken action accordingly. We have
10 made changes to address the majority of the issues raised by the reviewer.

11 **All the study is conducted on quartz microstructures, as also stated “we**
12 **focused on the microstructure of quartz-rich metamorphic rocks—quartz**
13 **is the main component of the rocks we collected and its deformation stress**
14 **is assumed to be representative of the region”, and those results are**
15 **extrapolated to be relevant for the unit. However, as presented in the**
16 **geological setting (methods section), the unit is composed by several rock**
17 **types with different compositions. Additionally, the quartz-rich**
18 **metasediments are composed of abundant mica. Even if a brief part of the**
19 **discussion considers this point, I think that it needs much more attention.**
20 **In this respect, the authors should also expand their citations, using**
21 **relevant literature discussing deformation mechanisms in quartz-rich**
22 **metasediments in subduction in other subduction zones, such as**
23 **Trepmann & Seybold, 2019 (<https://doi.org/10.1016/j.gsf.2018.05.002>),**
24 **Condit et al., 2022 (<https://doi.org/10.1029/2021GC010194>), Tulley et al.,**
25 **2020 (DOI: 10.1126/sciadv.aba1529), Giuntoli et al. 2022**
26 **(<https://doi.org/10.1029/2022JB024265>). Among others, those articles'**
27 **results and implications should be discussed. In particular, the role of**
28 **phyllosilicates in the bulk deformation needs much more attention, also**
29 **expanding on phase mixing between quartz and phengite (see for example**
30 **Hunter et al., 2016 <http://dx.doi.org/10.1016/j.jsg.2015.12.005>). The**
31 **discussion should be expanded in this regard.**

32

33 **Line 340: And what about the solution seams of Fig. 6a? Those seems to be**
34 **composed by phyllosilicates and are continuous. Please discuss this point**
35 **here**

36 Thank you for your comments regarding the deformation of quartz-rich
37 metasediments that also contain significant amounts of mica, and the presence
38 of several rock types with different compositions. After reading the
39 recommended literature we propose the following revisions.

40 In the quartz schist units targeted in this study, mica minerals are present and
41 may influence deformation. In our preprint, we wrote that mica does not
42 contribute to deformation because it does not form an interconnected network.
43 However, Hunter et al. (2016) pointed out that under a deformation temperature
44 of 490–530°C, even if they do not form an interconnected network, the
45 appearance of mica with a volume ratio of less than 10% may inhibit quartz
46 deformation and concentrate deformation in the mica. Furthermore, it has been
47 pointed out that the basal glide of phengite is weak and may undergo significant
48 deformation when the von Mises criterion is satisfied under deformation
49 conditions like our samples (Condit et al., 2022). In the light of these
50 considerations, we reassessed the effect of mica deformation and deformation
51 heterogeneity in rocks around our samples.

52 1. Rock around sample ASM2, 3, 4

53 When mica (relatively weak phase) grains do not form an interconnected
54 network, both the mica and quartz deform at the same strain rate and are
55 subjected to different stresses (mica distributed within a load-bearing quartz:
56 LBF in Handy (1994)). This condition applies to samples ASM2, 3, and 4. In this
57 situation, the estimated stresses would be larger than the stresses experienced
58 by the mica. However, the stress received by the whole rock body is, in this case,
59 the sum of the stress received by each mineral multiplied by the volume fraction
60 of the mineral (e.g., Condit et al., 2022; Handy, 1994). Thus, even if the mica is
61 subjected to a stress of 0 MPa and the volume fraction of the mica mineral is
62 20%, the stress on the rock body is 0.8 times the estimated stress and the
63 estimated stress can be considered to be a good approximation to the stress of
64 the whole rock body.

65 In summary, the estimated stresses are almost identical to the stresses received
66 by the surrounding rock body. However, the stresses received by the phengite
67 may be even smaller, as the strength of the mica is assumed to be lower than
68 the strength of the quartz undergoing dislocation creep at the temperature
69 conditions discussed in our study.

70 2. Rock around sample ASM1

71 It is likely that the obtained stress is considered to be largely representative of
72 the stresses undergone by the pelitic and psammitic schists of the chlorite zone.

73 2.1. Interpretation from outcrop and thin section observations

74 In the area around sample ASM1, both psammitic and pelitic schists are
75 deformed by quartz pressure solution creep in the microlithon domains, and the
76 developed foliation may have been deformed by phyllosilicate slip (Fig. 7a in
77 revised manuscript). As foliation develops as a layer, it is considered that the
78 foliation and microlithon domains are subjected to the same stress and
79 deformed at different strain rates (Condit et al., 2022). Both quartz veins (Fig. 7b
80 in revised manuscript; Fig. 2) and strain fringes (Fig. 7a in revised manuscript)
81 are developed in the microlithon domain, but no boudin or other structures
82 attributable to differences in strength could be identified (Fig. 7a in revised
83 manuscript; Fig. 2a). Therefore, quartz veins, strain fringes, and microlithon
84 domains are considered to have had almost the same strength, i.e, were
85 subjected to the same shear stress and strain rate.

86 In Sample ASM1, stresses were estimated from quartz veins in psammitic schist.
87 We also estimated shear stress experienced by strain fringes in the pelitic schist
88 (data will be added in the revised paper). From these results, we conclude it is
89 likely that the obtained stress is representative of the stresses undergone by the
90 pelitic and psammitic schists of the chlorite zone.

91 2.2. Interpretation from quartz rheology

92 2.2.1. Stress distribution

93 Estimated differential stresses were 32.3–71.7 MPa. In a quartz deformation
94 mechanism diagram drawn using the thin-film pressure solution creep flow law
95 (Table 1: Rutter, 1976; Schmidt and Platt, 2022) and dislocation creep flow law

96 (Table 1: Lusk et al., 2021), the conditions of the vein and fringe in sample ASM1
97 (Table 2: grain size = 20–35 μm ; the effective width of grain boundary = 0.339 μm
98 (no phyllosilicates)) is located at the dislocation creep deformation dominant
99 region (Fig. 1a), and microlithon domain condition (Table 2: grain size = 10–20
100 μm ; the effective width of grain boundary = 10.170 μm (presence of
101 phyllosilicates)) is located in the thin-film pressure solution creep dominant
102 region (Fig. 1b), consistent with geological observation. Therefore, the above
103 interpretation from outcrop and thin section observations is supported in terms
104 of quartz rheology.

105 2.2.2. Strain rate distribution

106 In this case, the strain rate of the microlithon domain is estimated to be twenty
107 times higher than that of dynamically recrystallized grains in the quartz vein and
108 fringe (Fig. 1). However, dynamically recrystallized grains in quartz vein and
109 fringe are considered to have been formed by the recrystallization of quartz fiber
110 grains that are elongated parallel to the stretching lineation (Fig. 7a in revised
111 manuscript; Fig. 2b). These fiber grains are formed associated with the opening
112 of the vein and the formation of the veins contributes to the strain of the rock.
113 Therefore, the strain rate experienced by the quartz veins and fringes is
114 considered to be the sum of the strain rate associated with the formation of
115 quartz fiber grains and the strain rate associated with quartz dislocation creep.
116 This additional contribution from dislocation creep may have allowed the quartz
117 vein and microlithon to deform at the same stress and strain rate.

118 The strain rate of thin-film pressure solution creep depends on grain size. Grain
119 size estimation using this method is difficult for structures with significant grain
120 growth inhibition by different minerals, and the grain size of the microlithon
121 domain used in the discussion is an assumption. Although this is not a problem
122 for rough strain rate comparisons such as the present study, an accurate grain
123 size estimation method is required for more quantitative strain rate evaluations.

124 2.3. Stress fluctuation

125 Trepmann & Seybold (2019) observed quartz veins that formed and developed
126 simultaneously with ductile deformation and documented microstructures
127 indicating dislocation glide and recrystallization associated with rapid stress

128 loading from the seismogenic zone and subsequent stress relaxation, as well as
129 the pressure solution creep of surrounding rock and opening and sealing of the
130 veins (crack-seal veins) associated with gradual internal stress loading and
131 subsequent stress relaxation. The structures observed in sample ASM1b area
132 are similar to the latter and may reflect multiple stages of stress concentration
133 and relaxation with a time interval of several hundred years (Trepmann &
134 Seybold 2019). In this case, the stress measured from the quartz vein in sample
135 ASM1 may be affected by a stress fluctuation. However, considering that
136 dynamic recrystallization requires strains of at least 0.2 (e.g., Stipp and Tullis,
137 2003) and that the calculated strain rate is approximately 10^{-13}s^{-1} , dynamically
138 recrystallized grains require at least 30,000 years to form. Therefore, the
139 influence of stress fluctuation over a period of a few hundred years can be
140 considered almost negligible.

141 2.4. Summary

142 In summary, we consider the obtained stress to be representative of the
143 stresses undergone by the surrounding pelitic and psammitic schists. Such
144 situations are only likely to occur when the deformation conditions are located
145 near the boundary between the dislocation creep domain and the pressure
146 solution creep domain. The change in the deformation mechanism between the
147 vein or fringe and microlithon domains can be attributed to differences in the
148 degree of grain growth inhibition and activation of pressure solution creep due
149 to the presence or absence of the quartz-mica boundary.

150

151

152

153

154

155

156

157

158

159

160

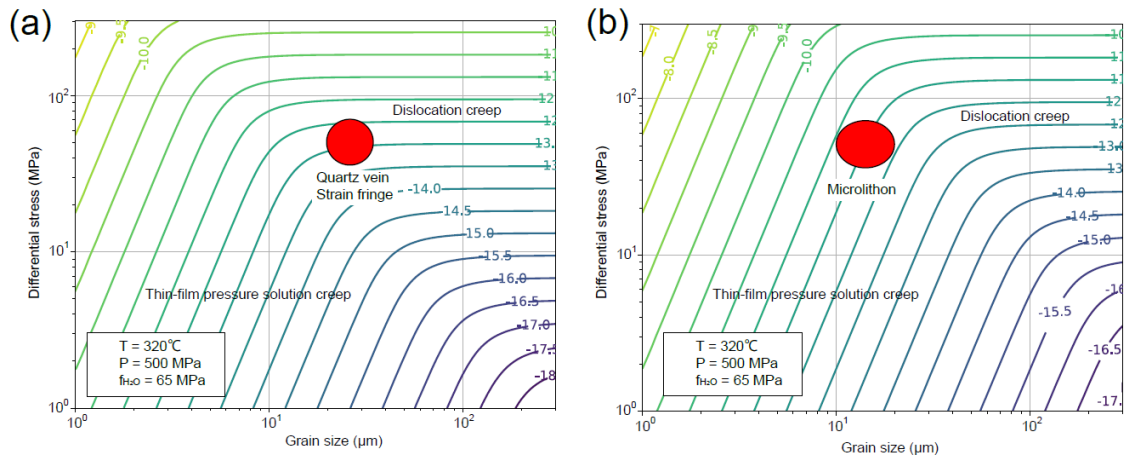
161

162

Formula	Description	Reference
$\dot{\varepsilon} = \frac{A_{ps} V_m c D_{gb} \omega \sigma \rho_f}{RT d^3 \rho_s}$	Thin film pressure solution flow law (s ⁻¹)	Rutter (1976) Schmidt and Platt (2021)
$\dot{\varepsilon} = A_{dsl}^{-9.3} f_{H_2O}^{0.49} \sigma^{3.5} \exp\left(-\frac{Q + PV}{RT}\right)$	Dislocation creep flow law (s ⁻¹)	Lusk et al. (2021)

163

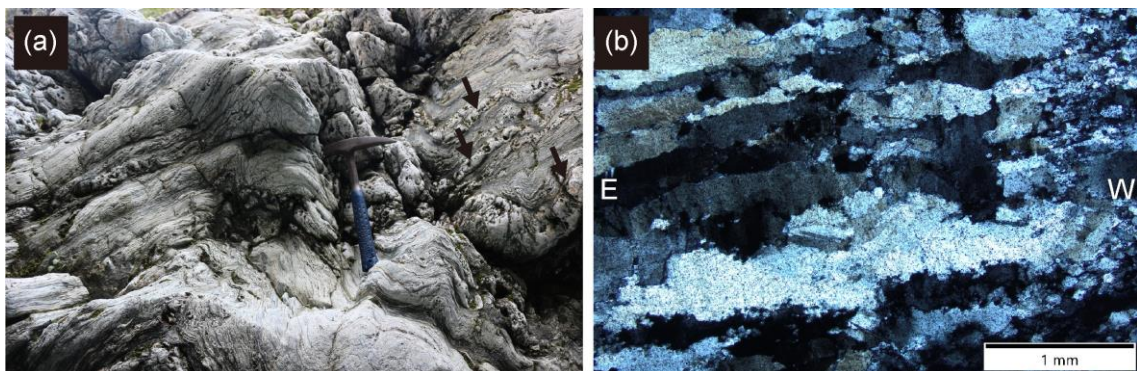
Parameter	Description	Value	Reference
A_{ps}	Geometric constant	44	Den Brok (1998)
V_m	Molar volume of solid (m ³ mol ⁻¹)	2.269×10 ⁻⁵	Berman (1988)
c	Solubility of solid in fluid phase (mole fraction)	2.954×10 ⁻²	Fournier and Potter (1982)
D_{gb}	Grain boundary diffusivity (m ² s ⁻¹)	7.00×10 ⁻²¹	Farver and Yund (1997)
ω	Effective width of grain boundary (μm)	0.339, 10.170	Dobe et al. (2021) Hickman and Evans (1995)
ρ_f	Density of fluid (kgm ⁻³)	1058	Burnham (1969)
ρ_s	Density of solid (kgm ⁻³)	2650	Schmidt and Platt (2022)
A_{dsl}	Geometric prefactor	10 ^{-7.9}	Lusk et al. (2021)
σ	Differential stress (uniaxial, MPa)	32.3–71.7	This study
f_{H_2O}	Water fugacity (MPa)	65	Holland and Powell (2004)
R	Gas constant (Jmol ⁻¹ K ⁻¹)	8.314	
T	Temperature (K)	593	This study
Q	Activation enthalpy (Jmol ⁻¹)	118000	Lusk et al. (2021)
P	Pressure (MPa)	500	This study
V	Activation volume (cm ³ mol ⁻¹)	2.45	Lusk et al. (2021)
d	Grain size (μm)	15, 20-35	This study



164

165 Figure 1: Deformation mechanism diagram of (a) quartz vein/strain fringe
 166 condition and (b) microlithon condition. The contour line indicates the
 167 exponential part of the strain rate (given for uniaxial conditions and needs to be
 168 multiplied by $\sqrt{3}$ if converting to simple shear strain rate (Lusk et al., 2021)).

169



170

171 Figure 2: (a) Outcrop photo showing foliation-subparallel veins (black arrows) in
 172 psammitic schist. Both foliation and veins were folded by later deformation (Du),
 173 but partly preserved unfolded structure, in which we collected sample ASM1b.
 174 (b) Microstructure of quartz vein (sample ASM1b). Large fibrous quartz grains
 175 that are elongated parallel to lineation and small recrystallized quartz grains
 176 were observed. XZ plane. Crossed nicols.

177

178

179

180 3. Deformation heterogeneity within different lithologies and stress in the
181 subduction plate interface

182 Tulley et al. (2020) compared the flow laws for various rocks with the strength
183 of hydrous metabasalt inferred from the geological structure and quartz
184 recrystallized grain size. The results showed that mica-containing
185 metasediments can be harder or softer than hydrous metabasalt or amphibolite,
186 depending on temperature conditions. It was also shown that the strength of
187 hydrous metabasalt is reduced by pressure solution creep and slip of
188 phyllosilicates, which plays an important role in deformation along the
189 subduction boundary. Therefore, the discussion of deformation other than
190 quartz, pelitic, and psammitic schist is important for the discussion of rock
191 deformation at subduction boundaries.

192 In this study, no microstructural observations or stress estimates of quartz
193 schist and basic schist in the chlorite zone, or pelitic and basic schist in the garnet
194 and albite zones have been made. However, previous studies showed that the
195 basic schist in the oligoclase biotite zone appears to be less affected by Ds
196 deformation than other rock bodies (e.g., Mori and Wallis., 2010), indicating that
197 the associated strain is smaller. In addition, the quartz schist in the garnet zone
198 has well-developed sheath folds (Wallis, 1990; Endo and Yokoyama, 2019), which
199 are not observed in the surrounding lithologies suggesting that the strain in the
200 quartz schist is particularly high. It is therefore possible that each rock body was
201 deformed at a different strain rate and may have been deformed at the same
202 stress. To investigate this, stress estimates should be made from the quartz
203 domains for each type of schist, and the strength relationship between the other
204 domains and the quartz domains in each schist should be investigated from
205 structural observations to constrain the deformation strength of each rock type.
206 If the flow laws of the constituent minerals are known, they may be combined to
207 estimate the deformation of the entire rock body (Condit et al., 2022). It is also
208 important to focus on lithological boundaries to confirm the presence or
209 absence of structures that are attributable to strength contrasts. These are
210 topics for future research.

211

212 *In the revised paper, Sec. 4.1 "Stress recorded by quartz microstructure and in the*
213 *subduction plate interface" in preprint was removed, and the above text, figures, and*
214 *tables were revised to fit in with the text of the paper and added as Sec. 5.2 "Stress*

215 *recorded by quartz microstructure and in the subduction plate interface” (line 506 to*
216 *608 in marked-up manuscript version). This text is placed after Sec. 5.1 “Tectonic*
217 *stage of sample deformation” because the deformation temperature of sample ASM1*
218 *was required for the above discussion.*

219 *Changes were also made to the Abstract (line 25 to 26 in marked-up manuscript*
220 *version) and Conclusion (line 759 to 761 in marked-up manuscript version) to reflect*
221 *changes in the text.*

222 **And what about the role of ultramafic rocks? These are not discussed, yet**
223 **present in the unit.**

224 **Line 350: And what about the role of ultramafic slivers?**

225 Shear zones by antigorite serpentinite exist at the boundary between mantle
226 wedge-derived serpentinite and pelitic schist (Kawahara et al., 2016). Although
227 the area examined in our study is on the oceanic plate side of the subduction
228 boundary region, it is possible that different minerals and different stress and
229 strain conditions existed on the overriding plate side. Further research is needed
230 on this as well.

231

232 *In the paper, the above text was added to Sec 5.2 “Stress recorded by quartz*
233 *microstructure and in the subduction plate interface” (line 609 to 612 in marked-up*
234 *manuscript version).*

235 **Along this line of thoughts, I think that the discussion needs to be**
236 **expanded considering the results obtained by similar studies conducted on**
237 **other orogens (differential strain rates and deformation mechanisms**
238 **related to deep slow earthquakes). Regarding the latter point, the**
239 **discussion states only “Therefore, the estimated stress may represent the**
240 **initial conditions from which slow earthquakes in the same domain**
241 **nucleated”.**

242

243 In Sample ASM1, traces of pressure solution creep and dislocation creep, such
244 as dynamically recrystallized grains in quartz veins and strain fringes in
245 microlithons, are visible. On the other hand, the partly recrystallized quartz
246 fibers in quartz veins (Fig. 2b) and phyllosilicate foliation suggest that brittle
247 deformation such as vein opening and phyllosilicate slip also occurred at the

248 same time. This indicates that the quartz vein was opened by nearly lithostatic
249 pore fluid pressure and fiber quartz grains were formed, followed by
250 recrystallization of these fiber grains, and repeating of this sequence in the rock
251 deformed by quartz pressure solution creep combined with slip along
252 phyllosilicates led to the formation of the present structure (Fig. 2a). Although
253 inclusion bands were not observed, this is a feature similar to crack-seal veins,
254 and the formation process is similar to the structures inferred by Giuntoil et al.
255 (2022) and Ujiie et al. (2018). In particular, it may be compared with the results
256 of the slow earthquakes study by Giuntoil et al. (2022), which suggests that
257 dislocation creep, pressure solution creep, phyllosilicate slip, and vein formation
258 caused slow earthquake cycles and associated fluid migration. The stress
259 estimates in Sample ASM1 are considered to be representative of the
260 surrounding rock body and may therefore be used as stress conditions at the
261 time that deep slow earthquakes were initiated. Compared with the differential
262 stresses and strain rates estimated from recrystallized quartz grains in Giuntoil
263 et al. (2022) (43 to 55 MPa (upper bond) and 10^{-14}s^{-1} to 10^{-13}s^{-1} (lower bond)), the
264 results from sample ASM1 (34.7 to 71.7 MPa and $10^{-11.4}\text{s}^{-1}$ to $10^{-11.8}\text{s}^{-1}$ in uniaxial
265 deformation, which must be multiplied by $\sqrt{3}$ for simple shear strain rate (Lusk
266 et al., 2021)) show higher strain rates. These differences may reflect the faster
267 strain rates in the Sanbagawa subduction zone, associated with rapid
268 subduction velocities (24 cm/yr).

269 As discussed above, Trepmann & Seybold (2019) observed pressure solution
270 creep of the surrounding rock and opening and sealing of the veins (crack-seal
271 veins) associated with gradual internal stress loading and subsequent stress
272 relaxation. The structures found in the ASM1 area are similar to these structures
273 and may reflect multiple stress concentrations and relaxations on a scale of
274 several hundred years. Whether this structure can generate slow earthquakes
275 may be constrained in terms of frequency, by examining the time scale of
276 formation of each vein, the number of veins, and the time scale taken to form
277 the entire vein seen in the outcrop.

278 *In the paper, Section 5.4 "Relationship with deep slow earthquakes" was prepared*
279 *according to the description above (line 682 to 722 in marked-up manuscript version).*

280

281 **More geological context is needed (see specific comments in the attached**
282 **PDF), in particular for the reader to picture the relation between the**
283 **different rock types and the relation between minerals marking the fabrics.**
284 **Additionally, could you add a figure with field photos (e.g. where these**
285 **samples were collected, main structures,...)**

286 *We added some geological context according to comments in the attached PDF. To*
287 *picture the relation between different rock types, we added geological cross section*
288 *to the geological map in Fig. 3 (line 212 to 215). To picture the relation between*
289 *minerals marking the fabrics, Sec.2 "Geological setting", Sec. 4 "Results" and Sec. 5*
290 *"Discussion" were revised according to comments. We also added some field photos*
291 *as Fig. 6a and Fig. S1 (supplement).*

292 **Finally, as EBSD was performed, please also show pole figures for the <a>**
293 **axis for all analysed samples and EBSD maps, such as grain size maps, KAM**
294 **maps, IPF maps. This is to improve documentation and to support your**
295 **interpretation of deformation mechanisms and grain size used for**
296 **piezometry.**

297 In addition to the <c> axis, pole figures for the <a> axis are added. Also,
298 mis2mean, KAM, and IPF Z maps were added as evidence for dislocation creep
299 and dynamic recrystallization. The results of grain boundary estimation and
300 selection of recrystallized grains, which are necessary to calculate grain size, are
301 shown for the case of substituting the piezometer of Cross et al. (2017) and the
302 case of substituting the piezometer of Shimizu (2012), respectively. In adding the
303 information, the analysis and interpretation of the results of Condit et al. (2022)
304 and Giuntoli et al. (2022) were very helpful. Thank you for recommending the
305 literature.

306
307 *Figures including optical microscope images, inverse pole figure map, mis2mean*
308 *maps, kernel average misorientation maps, grain boundary maps, and grain size*
309 *distribution maps were prepared and added to the paper. Due to its large size, it was*
310 *added as a supplement (Fig. S2 to S8), with the exception of sample ASM2XZ (Fig. 8).*
311 *Correspondingly, the text has also been changed (e.g., line 329 to 332 in marked-up*
312 *manuscript version).*

313

314 **Comment in pdf**

315 **Line 29: maybe better to approximate to 15-30 km?**

316 Thank you for pointing this out. *We have made the correction (line 30 in marked-up manuscript*
317 *version).*

318 **Line 77: What is the reference for this strain rate? For what geological setting? Please, specify**

319 If it is assumed that the plate motion causes the material in the plate boundary region to deform by
320 simple shear, and the thickness of the subduction zone is w (we assumed 100 m to 10 km) and the
321 subduction rate is v (we assumed 3cm per year), then the strain rate of rocks along the subduction
322 interface can be calculated as $v/w = 10^{-13} \text{ s}^{-1}$ to 10^{-11} s^{-1} .

323 *We have made the correction (line 79 to 84 in marked-up manuscript version).*

324

325 **Line 81: Specify here also the rock type**

326 Thank you for pointing this out. *We have made the corrections: quartz, pelitic, and psammitic schist*
327 *(line 88 to 89 in marked-up manuscript version).*

328 **Line 99: Is it common to have geological settings under method section? Please, check with journal**
329 **guidelines**

330 Thank you for pointing this out. *Sections 2.1 and 2.2 in preprint were titled “Geological setting” and*
331 *are removed from the Method.*

332

333 **Line 108: Please, specify rock types composing such unit. This applies for all units.**

334 Thank you for pointing this out. We have made the corrections:

335 According to Aoya et al. (2013b) and Endo and Yokoyama (2019),

336 **Eclogite unit:** pelitic schist, quartz (siliceous) schist, basic (mafic) schist, marble, pelitic-psammitic
337 gneiss, siliceous gneiss, mafic gneiss, metagabbro, diopside hornblende rock, and ultramafic rocks.
338 *(line 118 to 120 in marked-up manuscript version)*

339 **Kinouzu unit:** psammitic schist, pelitic schist, quartz(siliceous) schist, calcareous schist, and mafic
340 schist. *(line 113 to 114 in marked-up manuscript version)*

341 **Shirataki unit:** pelitic schist, psammitic schist, quartz (siliceous) schist, basic (mafic) schist,
342 metagabbro, and ultramafic rocks. *(line 123 to 124 in marked-up manuscript version)*

343 **Mikabu unit:** metachert, metabasalt, metagabbro, volcanioclastic rock, and ultramafic rocks. *(line*
344 *114 to 115 in marked-up manuscript version)*

345 **Oboke unit:** psammitic schist and pelitic schist. *(line 130 to 131 in marked-up manuscript version)*

346

347 **Line 113: Meaning what? Please specify**

348 We apologize for the confusing text. We have rewritten it as follows.

349 *“After the Eclogite unit was juxtaposed with the subducting Shirataki unit within the subduction*
350 *boundary, they underwent the same metamorphism at 89 to 85 Ma (Endo et al., 2012). This*
351 *metamorphism overprints the eclogite metamorphism and is referred to as the main metamorphic*
352 *stage.” (line 126 to 130 in marked-up manuscript version)*

353

354 **Line 115: Better metamorphic stage or event**

355 Thank you for pointing this out. *We have made the correction (line 130 in marked-up manuscript*
356 *version).*

357 **Line 118: As there are several stages, you need to specify for what stage this is valid**

358 We apologize for the confusing text. There are four metamorphic grades (zones). However, these four
359 metamorphic grades (zones) are the result of one metamorphism being subjected to different four
360 depth conditions.

361 *The text has therefore been amended as follows.*

362 *“The main metamorphism is divided into four metamorphic grades (Fig. 1) based on constituent*
363 *minerals in metapelite (Higashino, 1990).” (line 118 to 119 in preprint)*

364 *⇒”As a result of the main metamorphic stage, we can identify four metamorphic zones based on*
365 *constituent minerals in metapelite (Higashino, 1990; Fig. 1). These mineral zones can be related to*
366 *the depth to which the metamorphism occurred.” (line 134 to 137 in marked-up manuscript version)*

367

368 **Figure 1: Please, provide informations about the lithology not only for the eclogite unit, but for the**
369 **entire map. You could overlay info about metamorphic zonation on such map.**

370 Thank you for pointing this out. *Lithology information will be deleted, and a geological map of the*
371 *same area will be produced and placed side by side (Fig. 1b; line 150 to 155 in marked-up manuscript*
372 *version). As this study focuses on the shirataki unit, lithology other than the shirataki unit has been*
373 *omitted for simplicity of geological map.*

374 **Line 134: remove type**

375 Thank you for pointing this out. *We have made the correction. (line 156 in marked-up manuscript*
376 *version)*

377 **Line 135: What are the relations between those and the previous rock types?**

378 Thank you for pointing this out. *We added the following text.*

379 *“Ultramafic bodies are mantle wedge-derived rock bodies and differ in origin from schist derived from*
380 *subducted material. It is suggested that the rocks of garnet to oligoclase-biotite zone were subducted*
381 *to depths below the Moho boundary and the hanging-wall mantle became tectonically entrained in*
382 *these rocks (Aoya et al., 2013a).” (line 157 to 160 in marked-up manuscript version).*

383 **Line 136: Please, here specify again in what conditions this metamorphism took place**

384 **Line 137: Can you quickly summarize if this sequence has similar P-T conditions or not? Because**
385 **like this the reader has an idea of those abbreviations.**

386 **I see that you provide a few info in the figure, but please add also something here.**

387 The text has been amended as follows.

388 *“The main metamorphism that formed the Shirataki unit has four recognized ductile deformation*
389 *phases, named Dr, Ds, Dt, and Du deformation, respectively (Wallis, 1990; Fig. 2b, 2c).” (line 161 to*
390 *162 in marked-up manuscript version).*

391 *⇒” Each of the four metamorphic zones formed by the main metamorphic stage has a distinct P*
392 *(pressure)-T (temperature) path (Fig. 2a). Moreover, the rocks in all metamorphic zones show evidence*
393 *for four phases of ductile deformation, named Dr (burial), Ds (exhumation starting at near the peak*
394 *metamorphic conditions), Dt (exhumation after the peak metamorphic condition), and Du (slight*
395 *burial after exhumation) deformation, respectively (Wallis, 1990; Fig. 2b, 2c). Dt and Du are non-*
396 *penetrative and it is unlikely they had a major influence on exhumation or burial.” (line 162 to 167 in*
397 *marked-up manuscript version).*

398

399 **Line 141: I do not understand this sentence. Are the amphibole porphyroblasts zoned? What kind**
400 **of amphibole is? In what rock type?**

401 We apologize for the confusing text. The text has been revised as follows.

402 *“Compositional zoning of amphibole in and outside the porphyroblasts indicates that the Dr*
403 *deformation was formed during the subduction, burial phase (Wallis et al., 1992).” (line 170 to 171*
404 *in marked-up manuscript version).*

405 *⇒”The lack of compositional zoning of hornblende, barroisite, or glaucophane cores to actinolite-*
406 *winchite rims for grains of amphibole contained in the core of the albite porphyroblasts (preserving*
407 *Dr deformation features) in hematite-bearing metabasite indicates that the Dr deformation was*
408 *formed during the burial phase related to subduction (Wallis et al., 1992).” (line 172 to 174 in marked-*
409 *up manuscript version).*

410

411 **Fig. 2: Here you need to add P-T and time values.**

412 Thank you for your valuable comments. Deformation temperature pressure conditions vary according
413 to metamorphic grade, making it difficult to fill in specific values. Moreover, absolute time values are
414 not determined. Therefore, the text has been amended as follows:

415 *“(c) Main metamorphism P–T–D path of the Shirataki unit (Aoya, 2001) modified by Kouketsu et al.*
416 *(2021).” (line 188 to 189 in marked-up manuscript version).*

417 *⇒ “(c) Deformation phases in the Shirataki unit (after Kouketsu et al., 2021). This P-T path*

418 *corresponds to each metamorphic zone P-T path in the main metamorphism in Fig. 2a.*” (line 189 to
419 *190 in marked-up manuscript version).*

420 *The Fig. 2c was also modified to clarify the correspondence between Fig. 2a and Fig. 2c.*

421 **Line 154: Specify what kind of amphibole**

422 We apologize for the confusing text. The text has been revised as follows.

423 *“However, compositional changes of amphibole in the porphyroblasts and of Na-pyroxene in*
424 *equilibrium with albite of the garnet zone suggest that part of the Ds deformation occurred during a*
425 *pressure drop and temperature increase, i.e., before the peak metamorphic temperature was reached*
426 *(Wallis et al., 1992; Enami et al., 1994).”* (line 193 to 196 in marked-up manuscript version).

427 *⇒ “However, amphibole formed at highest temperatures (barroisite or hornblende) in the*
428 *porphyroblasts rim (formed during Ds deformation), and compositional changes of Na-pyroxene in*
429 *equilibrium with quartz and albite of the garnet zone suggest that part of the Ds deformation occurred*
430 *during a pressure drop and temperature increase, i.e., before the peak metamorphic temperature was*
431 *reached (Wallis et al., 1992; Enami et al., 1994).”* (line 196 to 199 in marked-up manuscript version).

432

433 **Line 169 to 172: This is sample description, not methods. Additionally, please describe all the rock**
434 **forming minerals of the sample**

435 The following revised text has been moved to the beginning of Sec. 4 “Results”:

436 *“Five samples were collected at four locations to obtain deformation information under a wide range*
437 *of temperature and pressure conditions (Fig. 3: ASM1–5). ASM1 is a sample from deformed quartz*
438 *veins, which are in psammitic schist and are oriented subparallel to the foliation, and samples ASM2–*
439 *5 are from quartz schist. Samples strongly affected by Dt or Du deformation were not used in this*
440 *study.”* (line 219 to 222 in marked-up manuscript version)

441 *⇒ “Five samples were collected at four locations to obtain deformation information under a wide*
442 *range of temperature and pressure conditions (Fig. 3). Samples strongly affected by Dt or Du*
443 *deformation were not used in this study. Sample ASM1b is from a deformed quartz vein, which is part*
444 *of a vein set developed in psammitic schist. The veins are oriented subparallel to the foliation (Fig.*
445 *6a). Sample ASM1a is from pelitic schist, and samples ASM2–5 are from quartz schist. The site where*
446 *sample ASM2-5 was collected was covered by vegetation and the outcrop is not well exposed (Fig.*
447 *S1). Psammitic schist and pelitic schist consist mainly of quartz, calcite, albite, phengite (Radvanec et*
448 *al., 1994), chlorite, and graphite. Quartz schist consists mainly of quartz, phengite (Radvanec et al.,*
449 *1994), albite, piemontite, ilmenite, and rutile.”*

450 *(line 316 to 322 in marked-up manuscript version)*

451

452 **Line 204 to 207: This paragraph I think that it is not needed, at least here, might be moved to**

453 **discussion**

454 Thank you for your valuable comments.

455 The relevant text has been deleted (*line 255 to 258 in marked-up manuscript version*).

456 In the following paragraphs, citations for BLG, SGR and GBM have been added (*line 259; line 274*
457 *to 275 in marked-up manuscript version*).

458

459 **Line 257: Please, state here what minerals define the foliation**

460 The text has been revised as follows.

461 (*line 323 to 325 in marked-up manuscript version*): “*The Ds foliation and stretching lineation of*
462 *psammitic and pelitic schist around sample ASMI is defined by pressure solution seams and quartz*
463 *strain fringes developed around pyrite observed in the surrounding area Fig. 3; Fig. 6a).*”

464 ⇒ “*Ds foliation and stretching lineation of psammitic and pelitic schist around sample ASMI is*
465 *defined by pressure solution seams consisting of phengite, chlorite, and graphite and quartz strain*
466 *fringes developed around pyrite (Fig. 3; Fig. 7a).*”

467

468 **Line 261: recrystallization?**

469 Thank you for pointing this out. We have made the correction (*line 332 in marked-up manuscript*
470 *version*).

471 **Line 265: call it phengite you must have chemical analyses.**

472 Thank you for pointing this out. We added a reference to chemical analyses. (Radvanec et al., 1994)
473 (*line 322 and 323 in marked-up manuscript version*).

474

475 **Line 328-330: This need to be moved to results section**

476 The following revised text has been moved to the Sec. 4 “results”:

477 “*In sample ASM2-4, albite includes traces of a Dr foliation oblique to the external Ds foliation which*
478 *is partly defined by the alignment of phengite. These observations suggest that both albite and phengite*
479 *were formed before or synchronously with Ds, the timing of quartz deformation. This implies that*
480 *albite and phengite have both been deformed along with the quartz.*”

481 (*line 329 to 332 in preprint ⇒ line 345 to 348 in marked-up manuscript version*).

482 The text of line 327 to 328 in preprint has been revised as follows.:

483 “*In Sample ASM2-4, in addition to quartz (volume fraction 70–80%: inferred by indexing rate of*
484 *EBSA analysis), albite and phengite are also significant mineral components (Fig. 6c–6f).*” (*line 327*
485 *to 328 in preprint*).

486 ⇒ “*In samples ASM2-4, in addition to quartz (volume fraction 70–80%: inferred by indexing rate of*
487 *EBSA analysis), albite and phengite are also significant mineral components, which deformed along*
488 *with quartz during Ds (Fig. 7c–7f).*” (*line 542 to 515 in marked-up manuscript version*).

489 **Line 342: This is a conference abstract not peer-reviewed. Please, find a better reference for this**
490 **concept.**

491 **They recently published an article**

492 **<https://www.sciencedirect.com/science/article/abs/pii/S0040195123000331?via%3Dihub>**

493 Thank you for pointing this out. We have removed the quotation from the relevant section when we
494 revised the text.

495

496 **Line 361: for what purpose?**

497 The text has been revised as follows.

498 *“The retrograde P-T gradient is the most important and this has been estimated as 0.3 GPa/100°C in*
499 *the albite-biotite zone and 0.4 GPa/100°C in the garnet and chlorite zones (Fig. 6d and 6f in Okamoto*
500 *and Toriumi, 2005).” (line 456 to 457 in marked-up manuscript version).*

501 *⇒“The retrograde P-T gradient is the most important to draw a retrograde P-T path, and this has*
502 *been estimated as 3 MPa K⁻¹ in the albite-biotite zone and 4 MPa K⁻¹ in the garnet and chlorite zones*
503 *(Fig. 6d and 6f in Okamoto and Toriumi, 2005).” (line 457 to 459 in marked-up manuscript version).*

504

505 **Line 398: Using the geothermal gradient provided above or the data from Enami et al., 2014? Please,**
506 **specify**

507 The text has been revised as follows.

508 *“Estimates for the pressures at which samples ASM1 and 3 were deformed are about 0.55±0.1 GPa*
509 *(21 km) and 0.7±0.2 GPa (27 Samples ASM2 and 4 were deformed at 0.45±0.1 GPa (17 km) and*
510 *0.5±0.1 GPa (19 km).” (line 497 to 499 in marked-up manuscript version).*

511 *⇒“Taking into consideration the peak pressure condition by Enami et al. (1994), the peak temperature*
512 *condition by Kouketsu et al. (2021), the retrograde P-T gradient by Okamoto and Toriumi (2005), and*
513 *estimated deformation temperature, pressures at which samples ASM1 and 3 were deformed are*
514 *estimated as 0.55 ± 0.1 GPa (21 km) and 0.7 ± 0.2 GPa (27 km). Samples ASM2 and 4 were deformed*
515 *at 0.45±0.1 GPa (17 km) and 0.5±0.1 GPa (19 km).“ (line 499 to 502 in marked-up manuscript version).*

516

517 **Line 406: Please, add a ref here**

518 We added references.

519 (e.g., Tagami and Takeshita, 1998) (line 617 to 618 in marked-up manuscript version).

520

521 **Line 477: All your samples, except 3. 1 does not count, as the T is inferred by the onset of SGR**

522 The text has been revised as follows.

523 *“In Fig. 9, the samples with blue circles are considered to have formed later in the exhumation process*
524 *than the other samples.” (line 724 to 725 in marked-up manuscript version).*

525 ⇒“In Fig. 9, the samples with blue circles are considered to have formed later in the exhumation
526 process than sample ASM3.” (line 724 to 725 in marked-up manuscript version).

527

528 **Line 481: Here I do not understand: those P estimates are linked to the deformation temperatures?**

529 **Please specify, also discussing how you extract those from the PO-T path**

530 The text has been revised as follows.

531 “Using the known P–T path we derived pressures for these samples of 0.7 ± 0.2 GPa (27 km) for ASM3,
532 0.5 ± 0.1 GPa (19 km) for ASM4, and 0.35 ± 0.1 GPa (13 km) for ASM5.” (line 731 to 732 in marked-up
533 manuscript version).

534 ⇒“Using the peak pressure condition by Enami et al. (1994), the peak temperature condition by
535 Kouketsu et al. (2021), the retrograde P–T gradient by Okamoto and Toriumi (2005), and estimated
536 deformation temperatures, we derived deformation pressure conditions for these samples of 0.7 ± 0.2
537 GPa (27 km) for ASM3, 0.5 ± 0.1 GPa (19 km) for ASM4, and 0.35 ± 0.1 GPa (13 km) for ASM5.” (line
538 727 to 730 in marked-up manuscript version).

539

540 **Line 494: Well, only sample 3, all the others are much lower than RCMT**

541 The text has been revised as follows.

542 “As shown in Fig. 9, many samples recorded deformation temperatures close to the peak and therefore
543 represent conditions close to the onset of exhumation.” (line 752 to 753 in marked-up manuscript
544 version).

545 ⇒“As shown in Fig. 9, there are few plots of deformation temperature conditions as low as ASM5,
546 and almost all data recorded deformation closer to the onset of exhumation.” (line 748 to 750 in
547 marked-up manuscript version).

548

549 **Line 494: But still within error, this is important to be stated here**

550 The text has been revised as follows.

551 “In contrast, the estimated differential (shear) stress of sample ASM5, which is the final recorded
552 stage of ductile deformation during ascent in this region, was found to increase significantly, ranging
553 from 92.8 to 127.1 MPa (46.4 to 63.6 MPa).” (line 750 to 752 in marked-up manuscript version).

554 ⇒“In contrast, the estimated differential (maximum shear) stress of sample ASM5, which is the final
555 recorded stage of ductile deformation during ascent in this region, are 92.8–127.1 MPa (46.4–63.6
556 MPa). This is a significant stress increase although the uncertainties in absolute estimates are large.”
557 (line 746 to 748 in marked-up manuscript version).

558

559 **Line 620 to 622: Can you cite a conference abstract? Please, check with journal rules**

560 Thank you for pointing this out. *The relevant citation has been deleted.*

561

562 **References**

563 Aoya, M.: P-T-D Path of Eclogite from the Sambagawa Belt Deduced from
564 Combination of Petrological and Microstructural Analyses, *J. Petrol.*, 42(7), 1225–
565 1248, 2001.

566 Aoya, M., Endo, S., Mizukami, T., and Wallis, S. R.: Paleo-mantle wedge preserved
567 in the Sambagawa high-pressure: Metamorphic belt and the thickness of forearc
568 continental crust, *Geology*, 41 (4), 451–454, doi:10.1130/G33834.1, 2013a.

569 Aoya, M., Noda, A., Mizuno, K., Mizukami, T., Miyachi, Y., Matsuura, H., Endo, S.,
570 Toshimitsu, and S., Aoki, M.: *Geology of the Niihama District. Quadrangle Series*
571 1:50,000, GSJ. AIST., Tsukuba, 2013b.

572 Berman, R. G.: Internally-Consistent Thermodynamic Data for Minerals in the
573 System Na₂O-K₂O-CaO-MgO-FeO-Fe₂O₃-Al₂O₃-SiO₂-TiO₂-H₂O-CO₂, *J. Petrol.*, 29 (2),
574 445–522, <https://doi.org/10.1093/petrology/29.2.445>, 1998.

575 Burnham, C. W., Holloway, J. R., and Davis, N. F.: The thermodynamic
576 properties of water to 1000°C and 10, 000 bars, *Geol Soc. Amer. Spec.*
577 *Paper*, pp.96, ISBN 13: 9780813721323, 1969.

578 Condit, C. B., French, M. E., Hayles, J. A., Yeung, L. Y., Chin, E. J., and Lee, C. A.:
579 Rheology of Metasedimentary Rocks at the Base of the Subduction Seismogenic
580 Zone, *Geochem. Geophys. Geosy.*, 23 (2), <https://doi.org/10.1029/2021GC010194>,
581 2022.

582 Cross, A. J., Prior, D. J., Stipp, M., and Kidder, S.: The recrystallized grain size
583 piezometer for quartz: An EBSD-based calibration, *Geophys. Res. Lett.*, 44 (13),
584 6667–6674, doi:10.1002/2017GL073836, 2017.

585 Den Brok, S. W. J.: Effect of microcracking on pressure-solution strain rate: The
586 Gratz grain-boundary model, *Geology*, 26 (10), 915–918,
587 [https://doi.org/10.1130/0091-7613\(1998\)026<0915:EOMOPS>2.3.CO;2](https://doi.org/10.1130/0091-7613(1998)026<0915:EOMOPS>2.3.CO;2), 1998.

588 Dobe, R., Das, A., Mukherjee, R., and Gupta, S.: Evaluation of grain boundaries as
589 percolation pathways in quartz-rich continental crust using Atomic Force
590 Microscopy, *Sci. Rep.*, 11 (1), 1–10, <https://doi.org/10.1038/s41598-021-89250-z>,
591 2021.

592 Enami, M., Wallis, S. R., and Banno, Y.: Paragenesis of sodic pyroxene-bearing
593 quartz schists: implications for the P-T history of the Sanbagawa belt, *Contrib.*
594 *Mineral. Petr.*, 116, 182–198, doi:10.1007/BF00310699, 1994.

595 Endo, S. and Yokoyama, S.: *Geology of the Motoyama District. Quadrangle Series*
596 *1:50,000*, Geol. Soc. Japan., Tsukuba, 2019.

597 Farver, J. and Yund, R.: Silicon diffusion in a natural quartz aggregate: constraints
598 on solution-transfer diffusion creep, *Tectonophysics*, 325 (3–4), 193–205,
599 [https://doi.org/10.1016/S0040-1951\(00\)00121-9](https://doi.org/10.1016/S0040-1951(00)00121-9), 2000.

600 Fournier, R. O. and Potter II, R. W.: An equation correlating the solubility of quartz
601 in water from 25° to 900°C at pressures up to 10,000 bars, *Geochim. Cosmochim.*
602 *Ac.*, 46 (10), 1969–1973, [https://doi.org/10.1016/0016-7037\(82\)90135-1](https://doi.org/10.1016/0016-7037(82)90135-1), 1982.

603 Giuntoil, F., Viola, G., and Sørensen, B. E.: Deformation Mechanisms of Blueschist
604 Facies Continental Metasediments May Offer Insights Into Deep Episodic Tremor
605 and Slow Slip Events, *J. Geophys. Res-Sol. Ea.*, 127 (10),
606 <https://doi.org/10.1029/2022JB024265>, 2022.

607 Handy, M. R.: Flow laws for rocks containing two non-linear viscous phases: A
608 phenomenological approach, *J. Struct. Geol.*, 16 (3), 287–301,
609 [https://doi.org/10.1016/0191-8141\(94\)90035-3](https://doi.org/10.1016/0191-8141(94)90035-3), 1994.

610 Hickman, S. H. and Evans, B.: Kinetics of pressure solution at halite-silica
611 interfaces and intergranular clay films, *J. Geophys. Res-Sol. Ea.*, 100 (87), 13113–
612 13132, <https://doi.org/10.1029/95JB00911>, 1995.

613 Holland, T. J. B. and Powell, R.: An internally consistent thermodynamic data set
614 for phases of petrological interest, *J. Metamorph. Geol.*, 16 (3), 309–343,
615 <https://doi.org/10.1111/j.1525-1314.1998.00140.x>, 2004.

616 Hunter N. J. R., Hasalová, P., Weinberg, R. F., and Wilson, C. J. L.: Fabric controls
617 on strain accommodation in naturally deformed mylonites: The influence of
618 interconnected micaceous layers, *J. Struct. Geol.*, 83, 180–193,
619 <https://doi.org/10.1016/j.jsg.2015.12.005>, 2016.

620 Kawahara, H., Endo, S., Wallis, S. R., Nagaya, T., Mori, H., and Asahara, Y., Brucite
621 as an important phase of the shallow mantle wedge: Evidence from the Shiraga
622 unit of the Sanbagawa subduction zone, SW Japan, *Lithos*, 254–255, 53–66,
623 <https://doi.org/10.1016/j.lithos.2016.02.022>, 2016.

624 Kouketsu, Y., Sadamoto, K., Umeda, H., Kawahara, H., Nagaya, T., Taguchi, T.,
625 Mori, H., Wallis, S., and Enami, M.: Thermal structure in subducted units from
626 continental Moho depths in a paleo subduction zone, the Asemigawa region of
627 the Sanbagawa metamorphic belt, SW Japan, *J. Metamorph. Geol.*, 39 (6), 727–
628 749, doi:10.1111/jmg.12584, 2021.

629 Lusk, A. D. J., Platt, J. P., and Platt, J. A.: Natural and Experimental Constraints on
630 a Flow Law for Dislocation-Dominated Creep in Wet Quartz, *J. Geophys. Res-Sol.*
631 *Ea.*, 126 (5), <https://doi.org/10.1029/2020JB021302>, 2021.

632 Mariani, E., Brodie, K. H., and Rutter, E. H.: Experimental deformation of
633 muscovite shear zones at high temperatures under hydrothermal conditions
634 and the strength of phyllosilicate-bearing faults in nature, *J. Struct. Geol.*, 28 (9),
635 1569–1587, doi:10.1016/j.jsg.2006.06.009, 2006.

636 Mori, H. and Wallis, R. S.: Large-scale folding in the Asemi-gawa region of the
637 Sanbagawa Belt, southwest Japan, *Isl. Arc.*, 19 (2), 357–370,
638 <https://doi.org/10.1111/j.1440-1738.2010.00713.x>, 2010.

639 Okamoto, A. and Toriumi, M.: Progress of actinolite-forming reactions in mafic
640 schists during retrograde metamorphism: An example from the Sanbagawa
641 metamorphic belt in central Shikoku, Japan, *J. Metamorph. Geol.*, 23 (5), 335–356,
642 doi:10.1111/j.1525-1314.2005.00580.x, 2005.

643 Radvanec, M., Banno, S., and Okamoto, K.: Multiple stages of phengite formation
644 in Sanbagawa schists, *Miner. Petrol.*, 51, 37–48, 1994.

645 Rutter, E., H.: A Discussion on natural strain and geological structure - The
646 kinetics of rock deformation by pressure solution, *Philos. T. R. Soc. A.*, 283 (1312),
647 203–219, <https://doi.org/10.1098/rsta.1976.0079>, 1976.

648 Schmidt, W. L. and Platt J. P.: Stress, microstructure, and deformation
649 mechanisms during subduction underplating at the depth of tremor and slow
650 slip, Franciscan Complex, northern California, *J. Struct. Geol.*, 154,
651 <https://doi.org/10.1016/j.jsg.2021.104469>, 2022.

652 Shimizu, I.: Steady-State Grain Size in Dynamic Recrystallization of Minerals, in:
653 Recrystallization, edited by Sztwiertnia, K., Intech, 371–386, doi:10.5772/33701,
654 2012.

655 Tagami, M. and Takeshita, T.: c-Axis fabrics and microstructures in quartz schist
656 from the Sambagawa metamorphic belt, central Shikoku, Japan, *J. Struct. Geol.*,
657 20 (11), 1549–1568, doi:10.1016/S0191-8141(98)00044-3, 1998.

658 Trepmann, C. A. and Seybold, L.: Deformation at low and high stress-loading
659 rates, *Geosci. Front.*, 10(1), 43–54, <https://doi.org/10.1016/j.gsf.2018.05.002>,
660 2019.

661 Tulley, C. J., Fagereng, A., and Ujiie, K.: Hydrous oceanic crust hosts megathrust
662 creep at low shear stresses, *Sci. Adv.*, 6(22), DOI: 10.1126/sciadv.aba1529, 2020.

663 Ujiie, K., Saishu, H., Fagereng, Å., Nishiyama, N., Otsubo, M., Masuyama, H., and
664 Kagi, H.: An Explanation of Episodic Tremor and Slow Slip Constrained by Crack-
665 Seal Veins and Viscous Shear in Subduction Mélange, *Geophys. Res. Lett.*, 45(11),
666 5371–5379, <https://doi.org/10.1029/2018GL078374>, 2018.

667 Wallis, S. R.: The timing of folding and stretching in the Sambagawa belt: The
668 Asemigawa region, central Shikoku, *J. Geol. Soc. Japan.*, 96(5), 345–352,
669 doi:10.5575/geosoc.96.345, 1990.

670 Wallis, S. R., Banno, S., and Radvanec, M.: Kinematics, structure and relationship
671 to metamorphism of the east-west flow in the Sanbagawa Belt, southwest Japan,
672 *Isl. Arc.*, 1(1), 176–185, doi:10.1111/j.1440-1738.1992.tb00068.x, 1992.

673

674 Reply to Referee Comment #2 (RC2)

675 Thank you for your feedback and suggested revisions. We appreciate your time
676 and effort in reviewing our preprint.

677 We have considered the comments and taken action accordingly. We have
678 made changes to address the majority of the issues raised by the reviewer.

679 **The manuscript carefully distinguishes various ductile deformation**
680 **stages and then focuses on the main deformation stage. This main stage,**
681 **however, represents early (and in one case late) exhumation. My concern**
682 **is to what extent shear stress during exhumation can be applied to rapid**
683 **subduction as the title suggests.**

684 Thank you for pointing this out. We have made the correction as follows:

685 The deformations we have studied were recorded during the early and late
686 stages of the exhumation. However, the orogen-oblique stretching lineation of
687 the D_s deformation is thought to reflect deformation closely related to rapid (24
688 cm/yr: Engebretson et al., 1985; Ishii & Wallis, 2020) and oblique subduction of
689 the subducted Izanagi Plate (e.g., Wallis, 1992; Wallis et al., 2009). For these
690 reasons we consider that the deformation under consideration formed as the
691 result of rapid subduction.

692 Moreover, if deformation of subducted sediments were driven by a
693 combination of Couette flow (simple shear) driven by the subducting plate, and
694 Poiseuille flow (channelized flow) driven by a pressure gradient produced by the
695 buoyancy of the subducted sediment (e.g., Fig.4 in Platt et al., 2018), it is possible
696 that exhumation of these rocks is associated with stable subduction. In this case,
697 what we observed can be the area close to the overriding plate within the plate
698 boundary domain.

699 *In the paper, additions have made to Sec. 2.2 "Deformation of Shirataki unit during*
700 *the main metamorphic stage" according to the description above. (line 206 to 209 in*
701 *marked-up manuscript version).*

702 **The authors focus only on the quartz-rich regions. As outlined in the**
703 **geological setting, the rocks are highly heterogeneous. The authors shortly**

704 **address the fact that ultramafic bodies are minor and can be neglected.**
705 **Even if so, figure 3 clearly shows that the quartz schists are not the major**
706 **lithology and that they are intercalated by pelitic and mafic schists. Such**
707 **heterogeneities can cause stress concentration and result in larger scale**
708 **stress gradients. Expanding the discussion in this direction as well as**
709 **discussing relevant literature is needed.**

710 Thank you for pointing this out. We have made the correction.

711 Tulley et al. 2020 compared the flow laws for various rocks with the strength of
712 hydrous metabasalt inferred from the geological structure and quartz
713 recrystallized grain size. The results showed that mica-containing
714 metasediments can be harder or softer than hydrous metabasalt or amphibolite,
715 depending on temperature conditions. It was also shown that the strength of
716 hydrous metabasalt is reduced by pressure solution creep and slip of
717 phyllosilicates, which plays an important role in deformation along the
718 subduction boundary. Therefore, the discussion of deformation other than
719 quartz schist, pelitic, and psammitic schist is important for the discussion of rock
720 deformation at subduction boundaries.

721 In this study, no microstructural observations or stress estimates of quartz
722 schist and basic schist in the chlorite zone, or pelitic and basic schist in the garnet
723 and albite zones have been made. However, previous studies showed that the
724 basic schist in the oligoclase biotite zone appears to be less affected by D_s
725 deformation than other rock bodies (e.g., Mori and Wallis., 2010), indicating that
726 the associated strain is smaller. In addition, the quartz schist in the garnet zone
727 has well-developed sheath folds (Wallis, 1990; Endo and Yokoyama, 2019), which
728 are not observed in the surrounding lithologies suggesting that the strain in the
729 quartz schist is particularly high. It is therefore possible that each rock body was
730 deformed at a different strain rate and may have been deformed at the same
731 stress. To investigate this, stress estimates should be made from the quartz
732 domains for each schist, and the strength relationship between the other
733 domains and the quartz domains in each schist should be investigated from
734 structural and textural observations to constrain the deformation strength of
735 each schist. If the flow laws of the constituent minerals are known, they may be
736 combined to estimate the deformation of the entire rock body (Condit et al.,
737 2022). It is also important to focus on lithological boundaries to confirm the

738 presence or absence of structures that are attributable to strength contrasts,
739 and this is a topic for future research.

740 Shear zones by antigorite serpentinite exist at the boundary between mantle
741 wedge-derived serpentinite and pelitic schist (Kawahara et al., 2016). Although
742 the area examined in our study is on the oceanic plate side of the subduction
743 boundary region, it is possible that different minerals and different stress and
744 strain conditions existed on the overriding plate side. Further research is needed
745 on this as well.

746 *In the revised paper, Sec. 4.1 "Stress recorded by quartz microstructure and in the*
747 *subduction plate interface" in preprint was removed, and the above text, figures, and*
748 *tables were revised to fit in with the text of the paper and added as Sec. 5.2.3*
749 *"Deformation heterogeneity within different lithologies and stress in the subduction*
750 *plate interface" (line 590 to 612 in marked-up manuscript version).*

751 **Furthermore, heterogeneities also occur on a micro scale. The**
752 **piezometers were applied to quartz-only domains. The authors argue that**
753 **the presence of sheet silicates inhibits grain growth and might cause**
754 **wrong estimates on differential stresses. The authors argue further that**
755 **sheet silicates do not form a network. However, in figure 6a it seems the**
756 **sheet silicates form a continuous layer. Again, such heterogeneities can**
757 **cause stress gradients. It would be interesting to see how much variation**
758 **in shear stress is obtained between quartz-only domains and more**
759 **heterogenous domains. And if significant these uncertainties should be**
760 **included into the discussion. Knowing that additional measurements need**
761 **time and effort, I think the manuscript would already benefit if these**
762 **points were addressed theoretically in the discussion.**

763 Thank you for your comments regarding the deformation of quartz-rich
764 metasediments that also contain significant amounts of mica. We propose the
765 following revisions.

766 ● Sample ASM2,3,4

767 The estimated stresses are almost identical to the stresses received by the rock
768 body. However, the stresses received by the mica minerals may be even smaller,

769 as the strength of the mica is assumed to be lower than the strength of the
770 quartz dislocation creep under the temperature conditions treated in our study.

771 Detail of the above discussion is stated in lines 40–69 of the reply comment for
772 RC1.

773 ● Sample ASM1

774 It is likely that the obtained stress is considered to be largely representative of
775 the stresses undergone by the pelitic and psammitic schists of the chlorite zone.
776 Such situations are only likely to occur when the deformation conditions are
777 located near the boundary between the dislocation creep domain and the
778 pressure solution creep domain. The change in the deformation mechanism
779 between the vein/fringe and microlithon domains can be attributed to the
780 difference in the degree of grain growth inhibition and activation of pressure
781 solution creep due to the presence or absence of the quartz-mica boundary.

782 Detail of the above discussion is stated in lines 70–149 of the reply comment for
783 RC1.

784 *In the revised paper, the above text, figures, and tables (lines 40–176 of the reply*
785 *comment for RC1) will be added as Sec. 5.2.1 “Stress recorded by sample ASM2, 3, 4*
786 *and stress received by surrounding quartz schist” and Sec. 5.2.2 “Stress recorded by*
787 *sample ASM1 and stress received by surrounding psammitic and pelitic schists”. (line*
788 *513 to 589 in marked-up manuscript version)*

789 **Line 70: “Shear stress is equal to half the differential stress.” Only the**
790 **maximum shear stress is equal to half the differential stress. Indeed, on**
791 **line 37 the author write that shear stress is used for absolute maximum**
792 **shear stress. I would suggest to strictly write maximum shear stress. The**
793 **data presented are estimates on the maximum shear stress and for the**
794 **discussion it is crucial to use accurate terms.**

795 Thank you for pointing this out. *We have made the correction (e.g., line 10 in*
796 *marked-up manuscript version).*

797 **Figure 1: the unit boundary of the smaller eclogite units is hardly**
798 **distinguishable from small ultramafic bodies. I suggest using different**

799 **colors for the boundary and the ultramafic bodies. (Actually, the color for**
800 **ultramafic bodies in figure 3 is different)**

801 *Thank you for pointing this out. Lithology information will be deleted, and a geological*
802 *map of the same area will be produced and placed side by side (Fig. 1b; line 151 to*
803 *155 in marked-up manuscript version). As this study focuses on the shirataki unit,*
804 *lithology other than the shirataki unit has been omitted for simplicity of geological*
805 *map.*

806 **Figure 2c: Can you add PT values here? Or otherwise plot the ductile**
807 **deformation stages in 2a.**

808 Thank you for your valuable comments. Deformation temperature pressure
809 conditions vary according to metamorphic grade, making it difficult to fill in
810 specific values. Therefore, the text has been amended as follows:

811
812 *“The main metamorphism that formed the Shirataki unit has four recognized ductile*
813 *deformation phases, named Dr, Ds, Dt, and Du deformation, respectively (Wallis,*
814 *1990; Fig. 2b, 2c).” (line 161 to 162 in marked-up manuscript version).*

815 *⇒ “Each of the four metamorphic zones formed by the main metamorphic stage has*
816 *a distinct P (pressure)-T (temperature) path (Fig. 2a). Moreover, the rocks in all*
817 *metamorphic zones show evidence for four phases of ductile deformation, named Dr*
818 *(burial), Ds (exhumation starting at near the peak metamorphic conditions), Dt*
819 *(exhumation after the peak metamorphic condition), and Du (slight burial after*
820 *exhumation) deformation, respectively (Wallis, 1990; Fig. 2b, 2c). Dt and Du are non-*
821 *penetrative and it is unlikely they had a major influence on exhumation or burial.”*
822 *(line 162 to 167 in marked-up manuscript version).*

823
824 *“(c) Main metamorphism P-T-D path of the Shirataki unit (Aoya, 2001) modified by*
825 *Kouketsu et al. (2021).” (line 188 to 189 in marked-up manuscript version).*

826 *⇒ “(c) Deformation phases in the Shirataki unit (after Kouketsu et al., 2021). This P-*
827 *T path corresponds to each metamorphic zone P-T path in the main metamorphism*
828 *in Fig. 2a.” (line 189 to 190 in marked-up manuscript version).*

829 *The Fig. 2c was also modified to clarify the correspondence between Fig. 2a and Fig.*
830 *2c.*

831 **Figure 4: Can you also add pole figures?**

832 Thank you for pointing this out. We have made the correction.

833 *Fig. 4 is related to Sec. 3.2 " Differential (maximum shear) stress estimation ", so it*
834 *has been added to Fig. 5, which is related to Sec. 3.3 "Deformation temperature*
835 *estimation by quartz c-axes fabric opening-angle thermometer ". (Fig. 5a in*
836 *marked-up manuscript version)*

837 **Table 3: The Cr+Ho data are a based on a corrected version of the Cross et**
838 **al. piezometer after Holyoke et al. This is only mentioned in the discussion**
839 **part. Please add some details also in the method section for better**
840 **understanding of the present table.**

841 Thank you for pointing this out. The following text has been added to the method
842 section.

843 *"We also used the piezometer of Cross et al. (2017) with a correction for measured*
844 *values by Griggs apparatus, which is proposed by Holyoke and Kronenberg (2010). In*
845 *this case, the stress value is 0.73 times the value obtained by piezometer of Cross et*
846 *al. (2017)."* (line 276 to 279 in marked-up manuscript version).

847

848 Once again, we sincerely appreciate the opportunity to address your comments
849 and concerns. If you have any further comments or queries, please do not
850 hesitate to contact us.

851 Yours sincerely

852 Authors.

853

854

855

856

857 **References**

- 858 Aoya, M.: P-T-D Path of Eclogite from the Sambagawa Belt Deduced from
859 Combination of Petrological and Microstructural Analyses, *J. Petrol.*, 42 (7), 1225–
860 1248, 2001.
- 861 Berman, R. G.: Internally-Consistent Thermodynamic Data for Minerals in the
862 System Na₂O-K₂O-CaO-MgO-FeO-Fe₂O₃-Al₂O₃-SiO₂-TiO₂-H₂O-CO₂, *J. Petrol.*, 29 (2),
863 445–522, <https://doi.org/10.1093/petrology/29.2.445>, 1998.
- 864 Burnham, C. W., Holloway, J. R., and Davis, N. F.: The thermodynamic
865 properties of water to 1000°C and 10, 000 bars, *Geol. Soc. Amer. Spec.*
866 *Paper*, pp.96, ISBN 13: 9780813721323, 1969.
- 867 Condit, C. B., French, M. E., Hayles, J. A., Yeung, L. Y., Chin, E. J., and Lee, C. A.:
868 Rheology of Metasedimentary Rocks at the Base of the Subduction Seismogenic
869 Zone, *Geochem. Geophys. Geosy.*, 23 (2), <https://doi.org/10.1029/2021GC010194>,
870 2022.
- 871 Cross, A. J., Prior, D. J., Stipp, M., and Kidder, S.: The recrystallized grain size
872 piezometer for quartz: An EBSD-based calibration, *Geophys. Res. Lett.*, 44 (13),
873 6667–6674, doi:10.1002/2017GL073836, 2017.
- 874 Den Brok, S. W. J.: Effect of microcracking on pressure-solution strain rate: The
875 Gratz grain-boundary model, *Geology*, 26 (10), 915–918,
876 [https://doi.org/10.1130/0091-7613\(1998\)026<0915:EOMOPS>2.3.CO;2](https://doi.org/10.1130/0091-7613(1998)026<0915:EOMOPS>2.3.CO;2), 1998.
- 877 Dobe, R., Das, A., Mukherjee, R., and Gupta, S.: Evaluation of grain boundaries as
878 percolation pathways in quartz-rich continental crust using Atomic Force
879 Microscopy, *Sci. Rep.*, 11 (1), 1–10, <https://doi.org/10.1038/s41598-021-89250-z>,
880 2021.
- 881 Endo, S. and Yokoyama, S.: *Geology of the Motoyama District. Quadrangle Series*
882 *1:50,000*, *Geol. Soc. Japan.*, Tsukuba, 2019.
- 883 Engebretson D. C., Cox A., and Gordon R. G.: Relative Motions Between Oceanic
884 and Continental Plates in the Pacific Basin, *Geol. Soc. Am.*, doi:10.1130/SPE206-
885 p1, 1985.

886 Farver, J. and Yund, R.: Silicon diffusion in a natural quartz aggregate: constraints
887 on solution-transfer diffusion creep, *Tectonophysics*, 325 (3–4), 193–205,
888 [https://doi.org/10.1016/S0040-1951\(00\)00121-9](https://doi.org/10.1016/S0040-1951(00)00121-9), 2000.

889 Fournier, R. O. and Potter II, R. W.: An equation correlating the solubility of quartz
890 in water from 25° to 900°C at pressures up to 10,000 bars, *Geochim. Cosmochim.*
891 *Ac.*, 46 (10), 1969–1973, [https://doi.org/10.1016/0016-7037\(82\)90135-1](https://doi.org/10.1016/0016-7037(82)90135-1), 1982.

892 Handy, M. R.: Flow laws for rocks containing two non-linear viscous phases: A
893 phenomenological approach, *J. Struct. Geol.*, 16 (3), 287–301,
894 [https://doi.org/10.1016/0191-8141\(94\)90035-3](https://doi.org/10.1016/0191-8141(94)90035-3), 1994.

895 Hickman, S. H. and Evans, B.: Kinetics of pressure solution at halite-silica
896 interfaces and intergranular clay films, *J. Geophys. Res-Sol. Ea.*, 100 (87), 13113–
897 13132, <https://doi.org/10.1029/95JB00911>, 1995.

898 Holland, T. J. B. and Powell, R.: An internally consistent thermodynamic data set
899 for phases of petrological interest, *J. Metamorph. Geol.*, 16 (3), 309–343,
900 <https://doi.org/10.1111/j.1525-1314.1998.00140.x>, 2004.

901 Holyoke, C. W. and Kronenberg, A. K.: Accurate differential stress measurement
902 using the molten salt cell and solid salt assemblies in the Griggs apparatus with
903 applications to strength, piezometers and rheology, *Tectonophysics*, 494 (1–2),
904 17–31, doi:10.1016/j.tecto.2010.08.001, 2010.

905 Hunter N. J. R., Hasalová, P., Weinberg, R. F., and Wilson, C. J. L.: Fabric controls
906 on strain accommodation in naturally deformed mylonites: The influence of
907 interconnected micaceous layers, *J. Struct. Geol.*, 83, 180–193,
908 <https://doi.org/10.1016/j.jsg.2015.12.005>, 2016.

909 Ishii, K. and Wallis, Simon. R.: High- and low-stress subduction zones recognized
910 in the rock record, *Earth. Planet. Sc. Lett.*, 531, doi:10.1016/j.epsl.2019.115935,
911 2020.

912 Kawahara, H., Endo, S., Wallis, S. R., Nagaya, T., Mori, H., and Asahara, Y., Brucite
913 as an important phase of the shallow mantle wedge: Evidence from the Shiraga
914 unit of the Sanbagawa subduction zone, SW Japan, *Lithos*, 254–255, 53–66,
915 <https://doi.org/10.1016/j.lithos.2016.02.022>, 2016.

916 Lusk, A. D. J., Platt, J. P., and Platt, J. A.: Natural and Experimental Constraints on
917 a Flow Law for Dislocation-Dominated Creep in Wet Quartz, *J. Geophys. Res-Sol.*
918 *Ea.*, 126 (5), <https://doi.org/10.1029/2020JB021302>, 2021.

919 Mariani, E., Brodie, K. H., and Rutter, E. H.: Experimental deformation of
920 muscovite shear zones at high temperatures under hydrothermal conditions
921 and the strength of phyllosilicate-bearing faults in nature, *J. Struct. Geol.*, 28 (9),
922 1569–1587, doi:10.1016/j.jsg.2006.06.009, 2006.

923 Mori, H. and Wallis, R. S.: Large-scale folding in the Asemi-gawa region of the
924 Sanbagawa Belt, southwest Japan, *Isl. Arc.*, 19 (2), 357–370,
925 <https://doi.org/10.1111/j.1440-1738.2010.00713.x>, 2010.

926 Platt, J. P., Xia, H., and Schmidt, W. L.: Rheology and stress in subduction zones
927 around the aseismic/seismic transition, *Prog. Earth Planet. Sci.*, 5 (24),
928 <https://doi.org/10.1186/s40645-018-0183-8>, 2018.

929 Rutter, E., H.: A Discussion on natural strain and geological structure - The
930 kinetics of rock deformation by pressure solution, *Philos. T. R. Soc. A.*, 283 (1312),
931 203–219, <https://doi.org/10.1098/rsta.1976.0079>, 1976.

932 Schmidt, W. L. and Platt J. P.: Stress, microstructure, and deformation
933 mechanisms during subduction underplating at the depth of tremor and slow
934 slip, Franciscan Complex, northern California, *J. Struct. Geol.*, 154,
935 <https://doi.org/10.1016/j.jsg.2021.104469>, 2022.

936 Tulley, C. J., Fagereng, A., and Ujiie, K.: Hydrous oceanic crust hosts megathrust
937 creep at low shear stresses, *Sci. Adv.*, 6 (22), DOI: 10.1126/sciadv.aba1529, 2020.

938 Wallis, S. R.: The timing of folding and stretching in the Sambagawa belt: The
939 Asemigawa region, central Shikoku, *J. Geol. Soc. Japan.*, 96 (5), 345–352,
940 doi:10.5575/geosoc.96.345, 1990.

941 Wallis, S. R.: Vorticity analysis in a metachert from the Sanbagawa Belt, SW Japan,
942 *J. Struct. Geol.*, 14 (3), 271–280, doi:10.1016/0191-8141(92)90085-B, 1992.

943 Wallis, S. R., Anczkiewicz, R., Endo, S., Aoya, M., Platt, J. P., Thirlwall, M., and Hirata,
944 T.: Plate movements, ductile deformation and geochronology of the Sanbagawa

945 belt, SW Japan: Tectonic significance of 89-88 Ma Lu-Hf eclogite ages, J.
946 Metamorph. Geol., 27 (2), 93-105, <https://doi.org/10.1111/j.1525->
947 1314.2008.00806.x, 2009.

948

949

950

951

952

953

954

955

956

957

958

959

960

961

962

963

964

965

966

967

968

969

970

971

972

973

974

975

976

977

978

979

980 **Other Changes**

981 The following amendments were made to improve the accuracy of the text.

982

983 *“Quartz grains in microlithon domain become finer due to grain growth inhibition by*
984 *different minerals such as phyllosilicates (Fig. 7a).” was added in line 333 to 335 in*
985 *marked-up manuscript version.*

986

987 *“Depth is calculated assuming thickness of granitic upper crust (2700kg m^{-3}) is 20 km*
988 *and that of gabbroic lower crust (3000kg m^{-3}) is 10 km.” was added in line 459 to 460*
989 *in marked-up manuscript version.*

990

991 *“Applied grain sizes were arithmetic mean and were calculated from the grain*
992 *boundaries for Shimizu (2012).” was added in line 662 to 663.*

993

994 *“Even taking these effects into account, the obtained stress values in this study are*
995 *greater than those of Takeshita (2021). This may be due to the fact that the EBSD-*
996 *based grain boundary estimation method makes it possible to consider smaller*
997 *grains.” was added in line 680 to 681 in marked-up manuscript version.*

998

999 *The text in Appendix B has been amended to supplement the relationship between*
1000 *dislocation density and grain size. (line 787 to 826 in marked-up manuscript version)*

1001

1002 *Fig. 4 was modified because the particles did not correspond between (c) the grain*
1003 *boundary map and (d) the grain size histogram.*

1004

1005 *Fig. 7 (d) (e) (f) and Fig. 10 have incorrect scales and have been corrected.*

1006

1007 *Tables 1, 2, and 3 were rewritten as new Tables 1 and 2.*

1008

1009 *To improve readability, the layout and the name of legends of Fig. 9 has been partially*
1010 *changed.*

1011

1012 *The layout of Table A1 has been changed.*

1013

1014 *To improve readability, the layout of Figs. 12, 13 and 14 have been partially changed.*
1015 *In addition, a numerical error in the error calculation was found (line 847 in marked-*

1016 *up manuscript version) and corrected.*

1017

1018 *Minor grammatical and expressive corrections were made in several other places.*